

## Electrostatically Driven CO– $\pi$ Aromatic Interactions

Ping Li,<sup>\*,†</sup> Erik C. Vik,<sup>†</sup> Josef M. Maier,<sup>†</sup> Ishwor Karki,<sup>†</sup> Sharon M. S. Strickland,<sup>‡</sup> Jessica M. Umana,<sup>‡</sup> Mark D. Smith,<sup>†</sup> Perry J. Pellechia,<sup>†</sup> and Ken D. Shimizu<sup>\*,†</sup>

<sup>†</sup>Department of Chemistry and Biochemistry, University of South Carolina, Columbia, South Carolina 29208, United States

<sup>‡</sup>Department of Biology, Chemistry, and Physics, Converse College, Spartanburg, South Carolina 29302, United States

### Supporting Information

**ABSTRACT:** A series of *N*-arylimide molecular balances were developed to study and measure carbonyl–aromatic (CO– $\pi$ ) interactions. Carbonyl oxygens were observed to form repulsive interactions with unsubstituted arenes and attractive interactions with electron-deficient arenes with multiple electron-withdrawing groups. The repulsive and attractive CO– $\pi$  aromatic interactions were well-correlated to electrostatic parameters, which allowed accurate predictions of the interaction energies based on the electrostatic potentials of the carbonyl and arene surfaces. Due to the pronounced electrostatic polarization of the C=O bond, the CO– $\pi$  aromatic interaction was stronger than the previously studied oxygen– $\pi$  and halogen– $\pi$  aromatic interactions.

Non-covalent interactions of aromatic surfaces play a key role in many chemistry, biology, and material science processes,<sup>1–4</sup> such as chemical reactivity and selectivity,<sup>5</sup> protein and DNA structure and function,<sup>6,7</sup> and supramolecular assembly.<sup>8</sup> A recent example is the interaction of carbonyl oxygens with aromatic surfaces.<sup>9–11</sup> Close contacts between carbonyl oxygens and the face of aromatic surfaces are frequently observed in crystal structure database surveys,<sup>11,12</sup> leading to the hypothesis that CO– $\pi$  aromatic interactions contribute to the structural stability and functioning of proteins and other biomacromolecules.<sup>13–16</sup> However, experimental studies measuring CO–arene interactions in solution have not been reported.<sup>17</sup> Therefore, the goal of this work is to systematically measure CO– $\pi$  aromatic interactions using a series of *N*-arylimide molecular balances to address three questions (Figure 1A): (1) Can carbonyl oxygens form stabilizing interactions with aromatic surfaces? (2) What are the strengths of these interactions? (3) Can we develop a predictive model for the interaction strengths?

The CO– $\pi$  interactions of aromatic surfaces were measured using six molecular balances, 1(CO)–6(CO) (Figure 1B). Restricted rotation of the *N*-aryl rotor sets up an equilibrium between *folded* and *unfolded* conformers in which the intramolecular CO– $\pi$  interactions are formed and broken. Thus, variations in the intramolecular interaction energies can be accurately measured via the *folded*–*unfolded* equilibrium. Our *N*-arylimide molecular balances have been successfully applied to a wide range of non-covalent interactions, including aromatic stacking,<sup>18–21</sup> heterocycle– $\pi$ ,<sup>22</sup> CH– $\pi$ ,<sup>23–27</sup> halogen– $\pi$ ,<sup>28,29</sup> chalcogen– $\pi$ ,<sup>30</sup> metal– $\pi$ ,<sup>31</sup> substituent– $\pi$ ,<sup>32</sup> and solvent

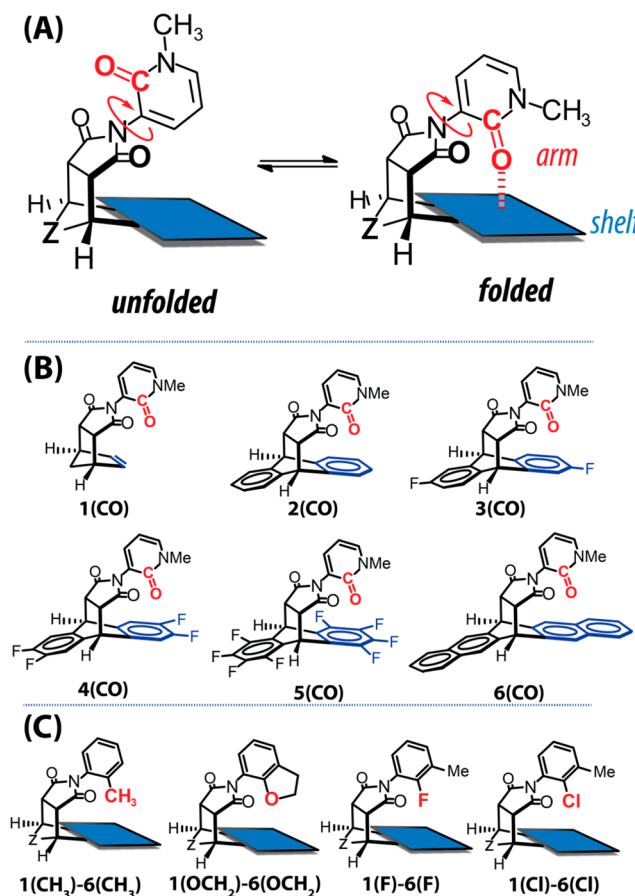


**Figure 1.** (A) *Folded*–*unfolded* equilibrium of the *N*-pyridin-2(1*H*)-onylimide molecular balances designed to measure the intramolecular CO–arene interactions in the *folded* conformation. (B) Structures of the carbonyl balances 1(CO)–6(CO) with six different arene shelves. (C) Abbreviated structures of four series of control balances with methyl (1(CH<sub>3</sub>)–6(CH<sub>3</sub>)), ether oxygen (1(OCH<sub>2</sub>)–6(OCH<sub>2</sub>)), fluorine (1(F)–6(F)), and chlorine (1(Cl)–6(Cl)) groups on the rotor that form intramolecular interactions with the same six arene shelves.

effects.<sup>33–37</sup> For balances 1(CO)–6(CO), the carbonyl group of the *N*-pyridin-2(1*H*)-onyl rotor is held in close proximity in the *folded* conformer over the face of an aromatic shelf. The size of the shelf increased from ethylene (1(CO)) to benzene

Received: June 14, 2019

Published: July 26, 2019

(2(CO)) to naphthalene (6(CO)). The electronic properties of the benzene shelf were also modulated by introducing zero (2(CO)), one (3(CO)), two (4(CO)), and four (5(CO)) fluorine substituents. In addition, four series of control balances were prepared with methyl (1(CH<sub>3</sub>)-6(CH<sub>3</sub>)), ether oxygen (1(OCH<sub>2</sub>)-6(OCH<sub>2</sub>)), fluorine (1(F)-6(F)), and chlorine (1(Cl)-6(Cl)) arms positioned over the same six aromatic shelves (Figure 1C).

The formation of intramolecular CO- $\pi$  interactions in the molecular balances was confirmed by X-ray crystallography. Only balance 5(CO) crystallized in the *folded* conformation, which was consistent with the strong stabilizing intramolecular CO- $\pi$  interaction in this balance (*vide infra*). The oxygen of the carbonyl group was positioned over the six-membered aromatic shelf (Figure 2) within van der Waals contact (<3.22 Å).<sup>11</sup> The

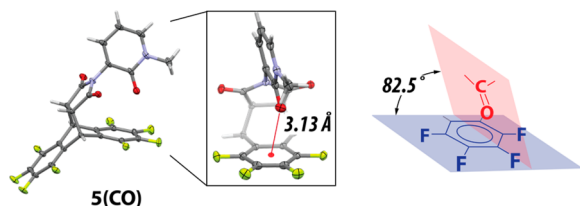


**Figure 2.** Side and front views of the X-ray crystal structure of balance 5(CO). The oxygen-to-centroid distance between the C=O arm and perfluorinated shelf is highlighted in red, and the dihedral angle between the planes of the CO group and arene shelf is illustrated on the right.

O-to-centroid distance (3.13 Å) and the dihedral angle (82.5°) between the arm carbonyl group and shelf six-membered ring were consistent with the previous crystal structure database surveys of CO- $\pi$  interactions (2.91–3.32 Å and 60–90°).<sup>9,11</sup> Balances 1(CO), 2(CO), 3(CO), 4(CO), and 6(CO) crystallized exclusively in the *unfolded* conformers (Supporting Information, Figure S1), which was consistent with their weaker or repulsive CO- $\pi$  interactions (*vide infra*).<sup>27</sup>

The folding ratios of the carbonyl balances were measured via integration of their <sup>1</sup>H or <sup>19</sup>F NMR spectra in CD<sub>3</sub>CN. The *folded* and *unfolded* conformers were in slow exchange at room temperature (23 °C) showing distinct sets of peaks. Integration of the *folded* and *unfolded* peaks provided an accurate measure of the *folded/unfolded* ratios ( $\leq 3\%$ ). In most cases, the *N*-methyl group on the rotor provided easily integratable singlets at 3.4 and 3.3 ppm. The *folded/unfolded* ratios were corroborated by monitoring multiple sets of peaks in the <sup>1</sup>H and <sup>19</sup>F NMR spectra. Similar stability trends for the carbonyl balances and control balances were observed in other organic solvents (CDCl<sub>3</sub>, CD<sub>2</sub>Cl<sub>2</sub>, acetone-*d*<sub>6</sub>, and DMSO-*d*<sub>6</sub>).

The CO- $\pi$  interaction energies were found to vary widely from destabilizing to stabilizing, depending on the nature of the aromatic surface (Figure 3, red bars). First, the CO- $\pi$  interactions with unsubstituted arene surfaces were destabilizing. Balances 2(CO) and 6(CO) with unfunctionalized benzene and naphthalene shelves favored the *unfolded* conformation and had large positive folding energies (1.44 and 1.11 kcal/mol). By comparison, balance 1(CO), which lacked an aromatic shelf, had a near unity folding ratio and a close to zero folding energy (0.26 kcal/mol). Second, and more interestingly, the CO- $\pi$  interactions became successively more stabilizing as electron-withdrawing fluorine substituents were added to the aromatic shelf (2(CO)–5(CO)). Balance 5(CO) with four fluorine substituents showed the most negative folding energy (–1.00

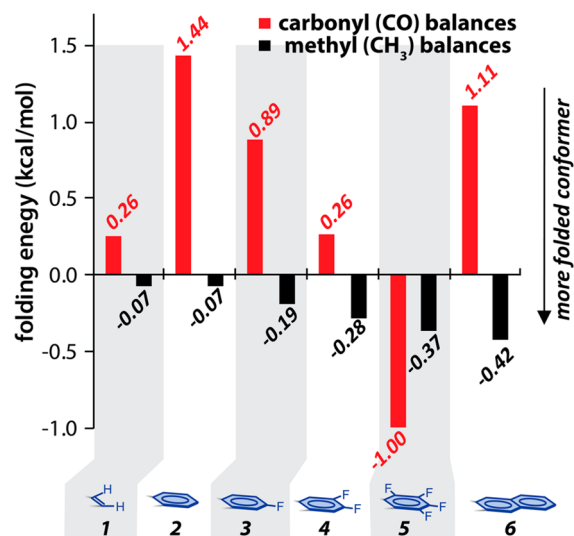


**Figure 3.** NMR-measured folding energies (CD<sub>3</sub>CN) of carbonyl (red bar) and methyl (black bar) arm balances with ethylene (1), benzene (2), fluorobenzene (3), difluorobenzene (4), tetrafluorobenzene (5), and naphthalene (6) shelves. Error in measured folding energy was less than  $\pm 0.02$  kcal/mol.

kcal/mol), which was consistent with an attractive CO- $\pi$  interaction. Third, extending the size of the aromatic shelf from benzene (2(CO)) to naphthalene (6(CO)) had only a small stabilizing effect ( $\Delta\Delta G = -0.33$  kcal/mol).

The importance of electrostatics to the CO- $\pi$  interaction was assessed via the methyl control balances (1(CH<sub>3</sub>)-6(CH<sub>3</sub>)) which positioned the CH<sub>3</sub> arm over the same six arene surfaces (Figure 3, black bars). The methyl arms form intramolecular CH- $\pi$  interactions<sup>38–40</sup> that are known to have a weak electrostatic component.<sup>41–43</sup> Unlike the carbonyl balances, the methyl balances did not show a large decrease in folding energy with increasing numbers of fluorine groups on the aromatic shelves. The overall change in folding energy ( $\Delta\Delta G$ ) for the methyl balances from the unsubstituted (2) to tetrafluoroarene shelf (5) was –0.30 kcal/mol in comparison to –2.44 kcal/mol for the carbonyl balances, which confirms the strong electrostatic nature of the CO- $\pi$  interaction.

Next, the electrostatic nature of the CO- $\pi$  interactions was quantitatively assessed by correlating the folding energies of the carbonyl and control balances with established electrostatic parameters. The electrostatic surface potential (ESP) at the center of the fluorinated arene shelves were calculated at the  $\omega$ B97X-D/6-31G\* level of theory (Figure 4 and Supporting Information, Figure S11). The ESP parameter has been successfully applied to study the electrostatic component of aromatic non-covalent interactions,<sup>44,45</sup> such as F- $\pi$ ,<sup>28</sup> cation- $\pi$ ,<sup>46</sup> and anion- $\pi$  interactions.<sup>47,48</sup> The folding energies of the carbonyl and methyl balances were correlated with the ESP values of the arene shelves with zero (2), one (3), two (4), and four fluorine (5) groups (Figure 4A,B). For both balance series, excellent linear correlations were observed ( $R^2 > 0.9$ ), demonstrating that the differences in the folding energies were strongly correlated to the electrostatic differences in the arene shelves. However, the slope of the shelf ESP correlation plot for the carbonyl balances ( $-7.79 \times 10^{-2}$ ) was eight times steeper than the methyl balances ( $-0.94 \times 10^{-2}$ ), indicating the much stronger electrostatic character of the CO- $\pi$  interaction versus the methyl-arene interaction. We also examined the possible

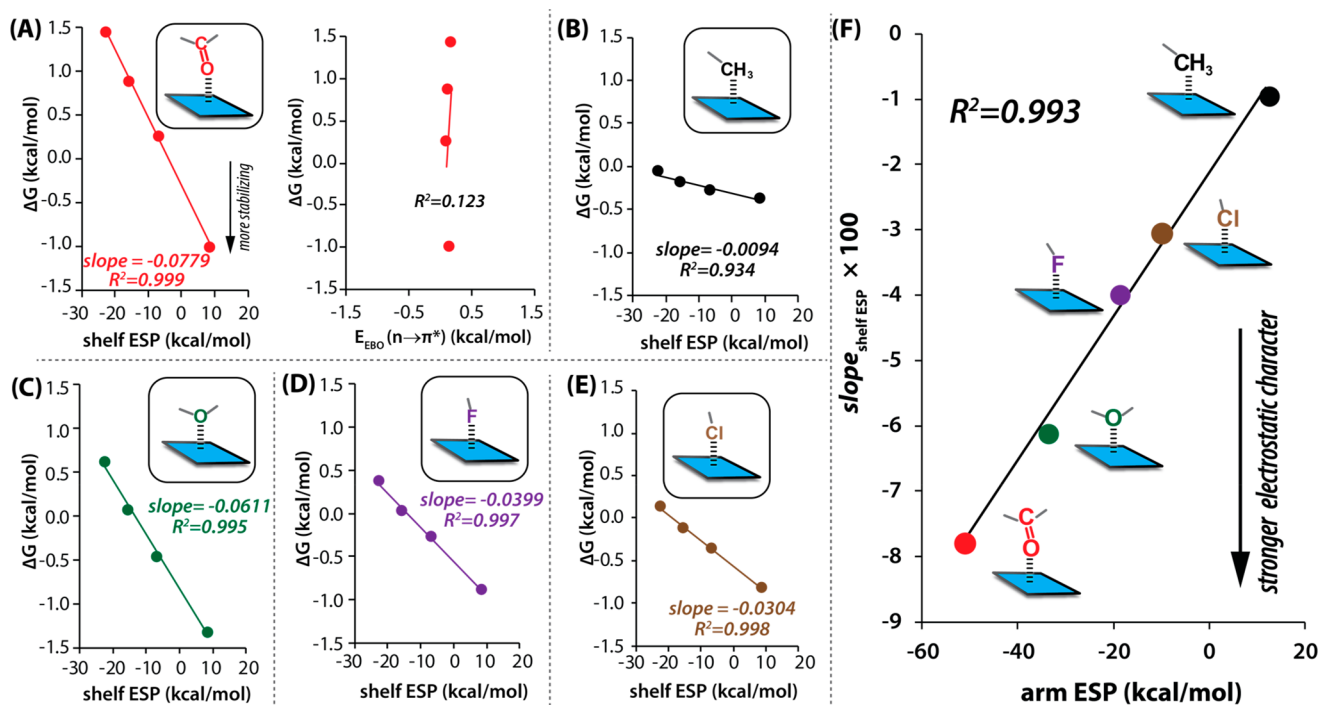


**Figure 4.** (A) Correlation plots of the measured folding energies ( $\Delta G$ , in  $\text{CD}_3\text{CN}$ ) of the carbonyl balances versus the calculated ESP values ( $\omega\text{B97X-D/6-31G}^*$ ) of the benzene shelves (2–5) with zero, one, two, and four fluorine substituents (left) and versus the calculated  $n \rightarrow \pi^*$  NBO energies ( $\omega\text{B97M-V/6-311G}^*$ ) between the CO and aromatic shelves (right). (B–E) Shelf ESP correlation plots for the methyl, ether, fluorine, and chlorine balances with progressively fluorinated benzene shelves (2–5). (F) Arm ESP correlation plot of the slopes of shelf ESP correlation plots ( $\text{slope}_{\text{shelf ESP}}$ ) for the five series of balances versus the calculated ESP values ( $\omega\text{B97X-D/6-31G}^*$ ) of their interacting region on the arm groups (CO,  $\text{CH}_3$ ,  $\text{OCH}_2$ , F, and Cl).

contribution of orbital–orbital interactions to the CO– $\pi$  aromatic interactions via NBO analysis.<sup>49</sup> The NBO orbital–orbital ( $n \rightarrow \pi^*$ ) energies did not show any correlation with the CO– $\pi$  interactions observed in balances 2(CO)–5(CO). The calculated NBO energies ( $\omega\text{B97M-V/6-311G}^*$ ) between the carbonyl oxygen lone pair ( $n$ ) and the aromatic shelf antibonding orbital ( $\pi^*$ ) were very small (0.10–0.17 kcal/mol). More importantly, the NBO energies ( $n \rightarrow \pi^*$ ) stayed relatively constant despite the observed CO– $\pi$  interaction varying widely from repulsive (with non-fluorinated benzene surface) to attractive (with tetrafluorobenzene surface).

Finally, the electrostatic component of CO– $\pi$  interactions was compared with other aromatic interactions using control balances that formed ether oxygen– $\pi$ <sup>50,51</sup> and halogen– $\pi$ <sup>28,29</sup> interactions. Specifically, the shelf ESP plots were measured for the ether (2( $\text{OCH}_2$ ))–5( $\text{OCH}_2$ )), fluorine (2(F))–5(F)), and chlorine (2(Cl))–5(Cl)) balances (Figure 4C–E). In each case, a linear correlation was observed. However, the slopes of each series differed and appeared to follow the size of the electrostatic term in the corresponding aromatic interactions. Therefore, the slopes of the shelf ESP correlation plots ( $\text{slope}_{\text{shelf ESP}}$ ) for each balance series (carbonyl, methyl, ether, fluorine, and chlorine) were correlated with the ESPs of the arm groups (CO,  $\text{CH}_3$ ,  $\text{OCH}_2$ , F, and Cl) interacting with the aromatic shelf in the folded conformer (Figure 4F). An excellent linear correlation ( $R^2 = 0.993$ ) was observed between the slopes of the shelf ESP plots ( $\text{slope}_{\text{shelf ESP}}$ ) versus the arm ESPs, confirming that the slope of the shelf ESP plots ( $\text{slope}_{\text{shelf ESP}}$ ) provides a measure of the magnitude of the electrostatic terms in each of these aromatic interactions. The slopes of the shelf ESP plots appear to effectively isolate the electrostatic component of the folding

energy from other factors such as sterics and solvophobic for each balance series, allowing accurate comparison of the different aromatic interactions.

Of the interactions compared in Figure 4F, the CO– $\pi$  had the strongest electrostatic component. Accordingly, the carbonyl (CO) balances also spanned the largest range ( $|\Delta\Delta G| = 2.44$  kcal/mol) of folding energies from destabilizing (1.44 kcal/mol) to stabilizing (–1.00 kcal/mol). By comparison, the ether ( $\text{OCH}_2$ ), fluorine (F), and chlorine (Cl) balance folding energies spanned narrower ranges ( $|\Delta\Delta G| = 1.96, 1.33,$  and 0.91 kcal/mol) due to their weaker electrostatic components. The oxygen in the ether ( $\text{OCH}_2$ ) balances also formed a fairly strong electrostatic interaction with the arene shelves. However, the CO– $\pi$  interaction was stronger due to the more polarized C=O bond. Other factors such as sterics, solvent effects, and dispersion also contributed to the folding energies as indicated by the differences in the  $y$ -intercepts of the shelf ESP correlation plots. For example, the ether balance (5( $\text{OCH}_2$ )) with the tetrafluorinated aromatic shelf is more folded than the corresponding carbonyl balance (5(CO)) due to the smaller destabilizing steric term that offsets the weaker attractive electrostatic term. However, the electrostatic component appears to be the dominant component of all these interactions as the ESPs of arm and shelf describes the majority of the observed folding energies.

In summary, the stability trends of CO– $\pi$  aromatic interactions were successfully measured in solution using our  $N$ -arylimide molecular balances. The interactions were repulsive for non-substituted aromatic surfaces and became systematically less repulsive as electron-withdrawing groups were added to the aromatic surface. For extremely electron poor aromatic surfaces,

the CO- $\pi$  aromatic interaction can be stabilizing, overcoming the inherent destabilizing steric interactions in our model system. These observations are consistent with crystal database studies which found oxygens tended to be over the center of electron poor heterocycles but over the edge of unsubstituted benzenes.<sup>11</sup> The interaction energy trends were well-correlated with the electrostatic parameter (ESP) of the interacting aromatic surface and the oxygen of the CO group. In this regard, the interaction behaves similar to an anion- $\pi$  interaction except involving a neutral but polarized oxygen. Based on the similarities in structure and ESP of the interacting groups in this model system, we expect that stabilizing CO- $\pi$  interactions of similar magnitude are present in synthetic and biological systems. For example, the ESP of the C=O of the *N*-pyridin-2(1*H*)-onyl rotor (-52.9 kcal/mol) is very similar to that of a peptide amide (-50.9 kcal/mol). On the other hand, the ESP of the C=O of acetone (-43.0 kcal/mol) and formaldehyde (-35.6 kcal/mol) is slightly smaller in comparison to the C=O of the *N*-pyridin-2(1*H*)-onyl rotor. Thus, ketone and aldehydes are expected to form weaker electrostatic CO- $\pi$  interactions. In addition, the ESP of the tetrafluorobenzene shelf (8.6 kcal/mol) is actually less positive than the ESP of thymine (14.5 kcal/mol), uracil (15.9 kcal/mol) and triazine (18.1 kcal/mol). The CO- $\pi$  interaction had a significantly larger electrostatic term than comparable ether O- $\pi$  or halogen- $\pi$  aromatic interactions, due to the strong polarization of the carbonyl bond, which leads to stronger stabilizing and destabilizing interactions. Finally, the CO- $\pi$  aromatic interactions appear to *not* arise from or be significantly stabilized by the orbital-orbital ( $n \rightarrow \pi^*$ ) interactions and thus should be treated differently from lone pair-carbonyl interactions,<sup>52</sup> which have been shown to have significant orbital-orbital contributions.

## ■ ASSOCIATED CONTENT

### Supporting Information

The Supporting Information is available free of charge on the ACS Publications website at DOI: 10.1021/jacs.9b06363.

Additional tables and figures, synthesis and characterization of molecular balances, measurements of folding energies, error analysis, calculations of electrostatic parameters and NBO energies, crystal structures, and <sup>1</sup>H, <sup>13</sup>C, and <sup>19</sup>F NMR spectra (PDF)

X-ray crystallographic data for 1(CO), 2(CO), 3(CO), 4(CO), 5(CO), 6(CO), 1(OCH<sub>2</sub>), 2(OCH<sub>2</sub>), 4(OCH<sub>2</sub>), 5(OCH<sub>2</sub>), and 6(OCH<sub>2</sub>) (CIF)

## ■ AUTHOR INFORMATION

### Corresponding Authors

\*li246@mailbox.sc.edu

\*shimizu@mail.chem.sc.edu

### ORCID

Ping Li: 0000-0001-9339-3111

Erik C. Vik: 0000-0003-1334-0293

Ken D. Shimizu: 0000-0002-0229-6541

### Notes

The authors declare no competing financial interest.

## ■ ACKNOWLEDGMENTS

Funding for this work was provided by the National Science Foundation, grant CHE 1709086.

## ■ REFERENCES

- (1) Meyer, E. A.; Castellano, R. K.; Diederich, F. Interactions with Aromatic Rings in Chemical and Biological Recognition. *Angew. Chem., Int. Ed.* **2003**, *42* (11), 1210–1250.
- (2) Salonen, L. M.; Ellermann, M.; Diederich, F. Aromatic Rings in Chemical and Biological Recognition: Energetics and Structures. *Angew. Chem., Int. Ed.* **2011**, *50* (21), 4808–4842.
- (3) Würthner, F.; Saha-Möller, C. R.; Fimmel, B.; Ogi, S.; Leowanawat, P.; Schmidt, D. Perylene Bisimide Dye Assemblies as Archetype Functional Supramolecular Materials. *Chem. Rev.* **2016**, *116* (3), 962–1052.
- (4) Aida, T.; Meijer, E. W.; Stupp, S. I. Functional Supramolecular Polymers. *Science* **2012**, *335* (6070), 813–817.
- (5) Yamada, S. Cation- $\pi$  Interactions in Organic Synthesis. *Chem. Rev.* **2018**, *118* (23), 11353–11432.
- (6) Burley, S. K.; Petsko, G. A. Aromatic-Aromatic Interaction - a Mechanism of Protein-Structure Stabilization. *Science* **1985**, *229* (4708), 23–28.
- (7) Hunter, C. A. Sequence-Dependent DNA-Structure - the Role of Base Stacking Interactions. *J. Mol. Biol.* **1993**, *230* (3), 1025–1054.
- (8) Chen, Z.; Lohr, A.; Saha-Möller, C. R.; Würthner, F. Self-assembled  $\pi$ -stacks of Functional Dyes in Solution: Structural and Thermodynamic Features. *Chem. Soc. Rev.* **2009**, *38* (2), 564–584.
- (9) Egli, M.; Sarkhel, S. Lone Pair-aromatic Interactions: To Stabilize or Not to Stabilize. *Acc. Chem. Res.* **2007**, *40* (3), 197–205.
- (10) Singh, S. K.; Das, A. The  $n \rightarrow \pi^*$  Interaction: A Rapidly Emerging Non-covalent Interaction. *Phys. Chem. Chem. Phys.* **2015**, *17* (15), 9596–9612.
- (11) Mooibroek, T. J.; Gamez, P.; Reedijk, J. Lone Pair- $\pi$  Interactions: A New Supramolecular Bond? *CrystEngComm* **2008**, *10* (11), 1501–1515.
- (12) Jain, A.; Purohit, C. S.; Verma, S.; Sankaramakrishnan, R. Close Contacts between Carbonyl Oxygen Atoms and Aromatic Centers in Protein Structures:  $\pi \cdots \pi$  or Lone-pair- $\pi$  Interactions? *J. Phys. Chem. B* **2007**, *111* (30), 8680–8683.
- (13) Gorske, B. C.; Bastian, B. L.; Geske, G. D.; Blackwell, H. E. Local and Tunable  $n \rightarrow \pi^*$  Interactions Regulate Amide Isomerism in the Peptoid Backbone. *J. Am. Chem. Soc.* **2007**, *129* (29), 8928–8929.
- (14) Jin, J.; He, B.; Zhang, X. Y.; Lin, H. N.; Wang, Y. SIRT2 Reverses 4-Oxononanoyl Lysine Modification on Histones. *J. Am. Chem. Soc.* **2016**, *138* (38), 12304–12307.
- (15) Rennie, M. L.; Doolan, A. M.; Raston, C. L.; Crowley, P. B. Protein Dimerization on a Phosphonated Calix[6]arene Disc. *Angew. Chem., Int. Ed.* **2017**, *56* (20), 5517–5521.
- (16) Gimenez, D.; Zhou, G.; Hurley, M. F. D.; Aguilar, J. A.; Voelz, V. A.; Cobb, S. L. Fluorinated Aromatic Monomers as Building Blocks To Control  $\alpha$ -Peptoid Conformation and Structure. *J. Am. Chem. Soc.* **2019**, *141* (8), 3430–3434.
- (17) Singh, S. K.; Mishra, K. K.; Sharma, N.; Das, A. Direct Spectroscopic Evidence for an  $n \rightarrow \pi^*$  Interaction. *Angew. Chem., Int. Ed.* **2016**, *55* (27), 7801–7805.
- (18) Carroll, W. R.; Pellechia, P.; Shimizu, K. D. A Rigid Molecular Balance for Measuring Face-to-face Arene-arene Interactions. *Org. Lett.* **2008**, *10* (16), 3547–3550.
- (19) Hwang, J.; Li, P.; Carroll, W. R.; Smith, M. D.; Pellechia, P. J.; Shimizu, K. D. Additivity of Substituent Effects in Aromatic Stacking Interactions. *J. Am. Chem. Soc.* **2014**, *136* (40), 14060–14067.
- (20) Hwang, J.; Dial, B. E.; Li, P.; Kozik, M. E.; Smith, M. D.; Shimizu, K. D. How Important Are Dispersion Interactions to the Strength of Aromatic Stacking Interactions in Solution? *Chem. Sci.* **2015**, *6* (7), 4358–4364.
- (21) Hwang, J.; Li, P.; Smith, M. D.; Shimizu, K. D. Distance-dependent Attractive and Repulsive Interactions of Bulky Alkyl Groups. *Angew. Chem., Int. Ed.* **2016**, *55* (28), 8086–8089.
- (22) Li, P.; Zhao, C.; Smith, M. D.; Shimizu, K. D. Comprehensive Experimental Study of *N*-Heterocyclic  $\pi$ -Stacking Interactions of Neutral and Cationic Pyridines. *J. Org. Chem.* **2013**, *78* (11), 5303–5313.

- (23) Carroll, W. R.; Zhao, C.; Smith, M. D.; Pellechia, P. J.; Shimizu, K. D. A Molecular Balance for Measuring Aliphatic CH- $\pi$  Interactions. *Org. Lett.* **2011**, *13* (16), 4320–4323.
- (24) Zhao, C.; Parrish, R. M.; Smith, M. D.; Pellechia, P. J.; Sherrill, C. D.; Shimizu, K. D. Do Deuteriums Form Stronger CH- $\pi$  Interactions? *J. Am. Chem. Soc.* **2012**, *134* (35), 14306–14309.
- (25) Zhao, C.; Li, P.; Smith, M. D.; Pellechia, P. J.; Shimizu, K. D. Experimental Study of the Cooperativity of CH- $\pi$  Interactions. *Org. Lett.* **2014**, *16* (13), 3520–3523.
- (26) Li, P.; Parker, T. M.; Hwang, J.; Deng, F.; Smith, M. D.; Pellechia, P. J.; Sherrill, C. D.; Shimizu, K. D. The CH- $\pi$  Interactions of Methyl Ethers as a Model for Carbohydrate-N-Heteroarene Interactions. *Org. Lett.* **2014**, *16* (19), 5064–5067.
- (27) Li, P.; Hwang, J.; Maier, J. M.; Zhao, C.; Kaborda, D. V.; Smith, M. D.; Pellechia, P. J.; Shimizu, K. D. Correlation between Solid-State and Solution Conformational Ratios in a Series of N-(o-Tolyl)-Succinimide Molecular Rotors. *Cryst. Growth Des.* **2015**, *15* (8), 3561–3564.
- (28) Li, P.; Maier, J. M.; Vik, E. C.; Yehl, C. J.; Dial, B. E.; Rickher, A. E.; Smith, M. D.; Pellechia, P. J.; Shimizu, K. D. Stabilizing Fluorine- $\pi$  Interactions. *Angew. Chem., Int. Ed.* **2017**, *56* (25), 7209–7212.
- (29) Sun, H.; Horatscheck, A.; Martos, V.; Bartetzko, M.; Uhrig, U.; Lentz, D.; Schmieder, P.; Nazare, M. Direct Experimental Evidence for Halogen-Aryl  $\pi$  Interactions in Solution from Molecular Torsion Balances. *Angew. Chem., Int. Ed.* **2017**, *56* (23), 6454–6458.
- (30) Hwang, J.; Li, P.; Smith, M. D.; Warden, C. E.; Sirianni, D. A.; Vik, E. C.; Maier, J. M.; Yehl, C. J.; Sherrill, C. D.; Shimizu, K. D. Tipping the Balance between S- $\pi$  and O- $\pi$  Interactions. *J. Am. Chem. Soc.* **2018**, *140* (41), 13301–13307.
- (31) Maier, J. M.; Li, P.; Hwang, J.; Smith, M. D.; Shimizu, K. D. Measurement of Silver- $\pi$  Interactions in Solution Using Molecular Torsion Balances. *J. Am. Chem. Soc.* **2015**, *137* (25), 8014–8017.
- (32) Hwang, J.; Li, P.; Vik, E. C.; Karki, I.; Shimizu, K. D. Study of Through-space Substituent- $\pi$  Interactions Using N-Phenylimide Molecular Balances. *Org. Chem. Front.* **2019**, *6* (8), 1266–1271.
- (33) Maier, J. M.; Li, P.; Vik, E. C.; Yehl, C. J.; Strickland, S. M. S.; Shimizu, K. D. Measurement of Solvent OH- $\pi$  Interactions Using a Molecular Balance. *J. Am. Chem. Soc.* **2017**, *139* (19), 6550–6553.
- (34) Maier, J. M.; Li, P.; Ritchey, J. S.; Yehl, C. J.; Shimizu, K. D. Anion-enhanced Solvophobic Effects in Organic Solvent. *Chem. Commun.* **2018**, *54* (61), 8502–8505.
- (35) Emenike, B. U.; Bey, S. N.; Bigelow, B. C.; Chakravartula, S. V. S. Quantitative Model for Rationalizing Solvent Effect in Noncovalent CH-Aryl Interactions. *Chem. Sci.* **2016**, *7* (2), 1401–1407.
- (36) Emenike, B. U.; Bey, S. N.; Spinelle, R. A.; Jones, J. T.; Yoo, B.; Zeller, M. Cationic CH $\cdots\pi$  Interactions as a Function of Solvation. *Phys. Chem. Chem. Phys.* **2016**, *18* (45), 30940–30945.
- (37) Emenike, B. U.; Spinelle, R. A.; Rosario, A.; Shinn, D. W.; Yoo, B. Solvent Modulation of Aromatic Substituent Effects in Molecular Balances Controlled by CH- $\pi$  Interactions. *J. Phys. Chem. A* **2018**, *122* (4), 909–915.
- (38) Takahashi, O.; Kohno, Y.; Nishio, M. Relevance of Weak Hydrogen Bonds in the Conformation of Organic Compounds and Bioconjugates: Evidence from Recent Experimental Data and High-Level *ab initio* MO Calculations. *Chem. Rev.* **2010**, *110* (10), 6049–6076.
- (39) Nishio, M.; Umezawa, Y.; Honda, K.; Tsuboyama, S.; Suezawa, H. CH/ $\pi$  Hydrogen Bonds in Organic and Organometallic Chemistry. *CrystEngComm* **2009**, *11* (9), 1757–1788.
- (40) Nishio, M.; Umezawa, Y.; Fantini, J.; Weiss, M. S.; Chakrabarti, P. CH- $\pi$  Hydrogen Bonds in Biological Macromolecules. *Phys. Chem. Chem. Phys.* **2014**, *16* (25), 12648–12683.
- (41) Ringer, A. L.; Figgs, M. S.; Sinnokrot, M. O.; Sherrill, C. D. Aliphatic C-H/ $\pi$  interactions: Methane-benzene, Methane-phenol, and Methane-indole Complexes. *J. Phys. Chem. A* **2006**, *110* (37), 10822–10828.
- (42) Tsuzuki, S.; Honda, K.; Fujii, A.; Uchimaru, T.; Mikami, M. CH/ $\pi$  Interactions in Methane Clusters with Polycyclic Aromatic Hydrocarbons. *Phys. Chem. Chem. Phys.* **2008**, *10* (19), 2860–2865.
- (43) Sherrill, C. D. Energy Component Analysis of  $\pi$  Interactions. *Acc. Chem. Res.* **2013**, *46* (4), 1020–1028.
- (44) Shimizu, K. D.; Li, P.; Hwang, J. Solution-Phase Measurements of Aromatic Interactions. *Aromatic Interactions: Frontiers in Knowledge and Application*; The Royal Society of Chemistry, 2017; Chap. 5, pp 124–171.
- (45) Hwang, J.; Li, P.; Shimizu, K. D. Synergy between Experimental and Computational Studies of Aromatic Stacking Interactions. *Org. Biomol. Chem.* **2017**, *15* (7), 1554–1564.
- (46) Dougherty, D. A. The Cation- $\pi$  Interaction. *Acc. Chem. Res.* **2013**, *46* (4), 885–893.
- (47) Berryman, O. B.; Johnson, D. W. Experimental Evidence for Interactions between Anions and Electron-deficient Aromatic Rings. *Chem. Commun.* **2009**, No. 22, 3143–3153.
- (48) Berryman, O. B.; Bryantsev, V. S.; Stay, D. P.; Johnson, D. W.; Hay, B. P. Structural Criteria for the Design of Anion Receptors: The Interaction of Halides with Electron-deficient Arenes. *J. Am. Chem. Soc.* **2007**, *129* (1), 48–58.
- (49) Weinhold, F. Natural Bond Orbital Analysis: A Critical Overview of Relationships to Alternative Bonding Perspectives. *J. Comput. Chem.* **2012**, *33* (30), 2363–2379.
- (50) Aliev, A. E.; Arendorf, J. R. T.; Pavlakos, I.; Moreno, R. B.; Porter, M. J.; Rzepa, H. S.; Motherwell, W. B. Surfing  $\pi$  Clouds for Noncovalent Interactions: Arenes versus Alkenes. *Angew. Chem., Int. Ed.* **2015**, *54* (2), 551–555.
- (51) Pavlakos, I.; Arif, T.; Aliev, A. E.; Motherwell, W. B.; Tizzard, G. J.; Coles, S. J. Noncovalent Lone Pair(No- $\pi!$ )-Heteroarene Interactions: The Janus-Faced Hydroxy Group. *Angew. Chem., Int. Ed.* **2015**, *54* (28), 8169–8174.
- (52) Newberry, R. W.; Raines, R. T. The n $\rightarrow\pi^*$  Interaction. *Acc. Chem. Res.* **2017**, *50* (8), 1838–1846.